NONLINEAR DYNAMIC MODEL FOR FLEXURAL VIBRATIONS ANALYSIS OF A SUPERCRITICAL HELICOPTER'S TAIL ROTOR DRIVE SHAFT

Zbigniew Dzygadlo and Witold Perkowski
Institute of Aviation, Al. Krakowska 110/114
02-256 Warsaw, Poland

Keywords: *helicopters tail rotor drive shaft, nonlinear dynamic model, flexural vibrations analysis*

Abstract

In the new ultra-light helicopter, just now designed in the Institute of Aviation, a light-weight supercritical tail rotor drive shaft will be used. This paper presents a nonlinear dynamic model of such a shaft for the analysis of its flexural vibrations.

The model assumes that the shaft has several deformable supports with elastic and damping elements and is loaded by external forces caused by its local unbalance.

The equations of motion have been obtained making use of the finite element method and dividing the shaft into several elements between successive supports.

In order to ensure easy crossing through a resonance region, a nonlinear dry friction damper has been applied in the shaft structure. Depending on the parameters of this damper, we can obtain various bending vibrations of the shaft under consideration. There can be regular or chaotic vibrations of the shaft.

1. Introduction

The dynamics of a supercritical tail rotor drive shaft is an interesting nonlinear problem of easy crossing through a resonance region [1]-[6].

The dynamic model considered in this paper assumes that the shaft is a continuous structure having several deformable supports with elastic and damping elements and is loaded by external forces caused by its local unbalance [1]-[3], [6].

The equations of motion have been determined by making use of the finite element method. Displacements of elements axes have been obtained by means of Hermite's polynomials and elements with four degrees of freedom have been determined in every of both considered planes [6].

Equations of motion of particular elements obtained from the virtual work principle, have been transformed into complex form and matrix equation of the whole shaft structure has been obtained including shaft supports.

A nonlinear dry friction damper has been applied in the shaft structure to ensure easy crossing through the resonance region. Depending on the parameters of the damper, various bending vibrations of the shaft can be obtained, which can be regular or chaotic ones [4], [5].

2. Equations of the Problem

Let us consider a supercritical tail rotor drive shaft moving with variable angular speed Ω and composed of a structure with continuous mass and elasticity distribution, having several deformable supports with elastic and damping elements and loaded by external forces caused by its local unbalance (Fig.1).

The equations of shaft motion can be obtained in a fixed orthogonal system of coordinates *0xyz* where the *x*-axis determines the position of a non-deformable shaft axis.

The equations of shaft motions will be developed making use of the finite element method and Hermite's polynomials for describing displacements of an element axis.
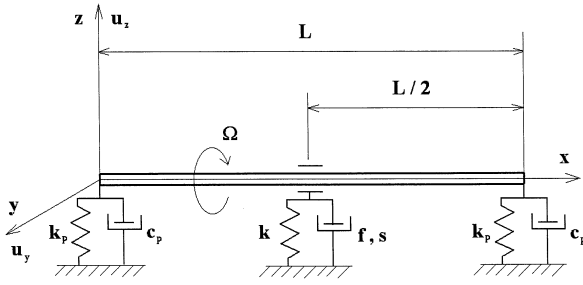
Fig.1. Sketch of the shaft.

By way of example we can show the equations of motion for a j-finite element

$$\mathbf{B}_j\ddot{\boldsymbol{\delta}}_{yj} + \mathbf{c}_j\dot{\boldsymbol{\delta}}_{yj} + \Omega\mathbf{I}_{oj}\dot{\boldsymbol{\delta}}_{zj} + \mathbf{K}_j\boldsymbol{\delta}_{yj} = \mathbf{F}_{eyj} + \mathbf{F}_{exyj}$$
$$\mathbf{B}_j\ddot{\boldsymbol{\delta}}_{zj} + \mathbf{c}_j\dot{\boldsymbol{\delta}}_{zj} - \Omega\mathbf{I}_{oj}\dot{\boldsymbol{\delta}}_{yj} + \mathbf{K}_j\boldsymbol{\delta}_{zj} = \mathbf{F}_{ezj} + \mathbf{F}_{exzj} \qquad (1)$$

where

$$\boldsymbol{\delta}_{yj} = \boldsymbol{\delta}_{yj}(t) = \left(u_{yj-1}, \theta_{yj-1}, u_{yj}, \theta_{yj}\right)^T$$
$$\boldsymbol{\delta}_{zj} = \boldsymbol{\delta}_{zj}(t) = \left(u_{zj-1}, \theta_{zj-1}, u_{zj}, \theta_{zj}\right)^T \qquad (2)$$

are examples of the displacement vectors of j-finite element in the yx and zx planes, and $u_{yj-1}, u_{yj}, u_{zj-1}, u_{zj}$ are dimensionless displacements, which are referred to L-length of the shaft, while $\theta_{yj-1}, \theta_{yj}, \theta_{zj-1}, \theta_{zj}$ are angles of rotations of both edges of j-finite element in yx and zx planes.

$\mathbf{B}_j = \mathbf{m}_j + \mathbf{I}_{1j}$; $\mathbf{I}_{oj}$ are inertial matrices,

$\mathbf{c}_j$ is external damping matrix

$\mathbf{K}_j$ is stiffness matrix,

$\mathbf{F}_{eyj}, \mathbf{F}_{ezj}$ are edge forces vectors and

$$\mathbf{F}_{exyj} = \mathbf{P}_{oj}\left[\Omega^2\cos(\Omega t) + \frac{d\Omega}{dt}\sin(\Omega t)\right]$$
$$\mathbf{F}_{exzj} = \mathbf{P}_{oj}\left[\Omega^2\sin(\Omega t) - \frac{d\Omega}{dt}\cos(\Omega t)\right] \qquad (3)$$

are external, unbalance forces vectors, $\mathbf{P_{oj}}$ is vector of the amplitude of unbalance forces.

If we introduce a complex vector of the element displacements

$$\boldsymbol{\delta}_{cj} = \boldsymbol{\delta}_{yj} + i\boldsymbol{\delta}_{zj}$$
$$u_{cj} = u_{yj} + iu_{zj} \qquad (4)$$
$$\theta_{cj} = \theta_{yj} + i\theta_{zj}$$

Eqs. (1) can be presented in the complex form

$$\mathbf{B}_j\ddot{\boldsymbol{\delta}}_{cj} + \left(\mathbf{c}_j - i\Omega\mathbf{I}_{oj}\right)\dot{\boldsymbol{\delta}}_{cj} + \mathbf{K}_j\boldsymbol{\delta}_{cj} = \mathbf{F}_{ecj} + \mathbf{F}_{excj} \qquad (5)$$

where

$$\mathbf{F}_{ecj} = \mathbf{F}_{eyj} + i\mathbf{F}_{ezj} \qquad (6)$$

$$\mathbf{F}_{excj} = \mathbf{P}_{oj}\left(\Omega^2 - i\frac{d\Omega}{dt}\right)e^{i\Omega t} \qquad (7)$$

If we make the sum by adding together Eqs. (1) or (5) for $j = 1,2,..,n$, where n is the number of finite elements into which the shaft is divided, we obtain the matrix equations of the whole shaft structure.

$$\mathbf{B}\ddot{\boldsymbol{\delta}}_y + \mathbf{c}\dot{\boldsymbol{\delta}}_y + \Omega\mathbf{I}_o\dot{\boldsymbol{\delta}}_z + \mathbf{K}\boldsymbol{\delta}_y = \mathbf{F}_{ey} + \mathbf{F}_{exy}$$
$$\mathbf{B}\ddot{\boldsymbol{\delta}}_z + \mathbf{c}\dot{\boldsymbol{\delta}}_z - \Omega\mathbf{I}_o\dot{\boldsymbol{\delta}}_y + \mathbf{K}\boldsymbol{\delta}_z = \mathbf{F}_{ez} + \mathbf{F}_{exz} \qquad (8)$$

or in the complex form

$$\mathbf{B}\ddot{\boldsymbol{\delta}}_c + \left(\mathbf{c} - i\Omega\mathbf{I}_o\right)\dot{\boldsymbol{\delta}}_c + \mathbf{K}\boldsymbol{\delta}_c =$$
$$= \mathbf{F}_{ec} + \mathbf{P}_o\left(\Omega^2 - i\frac{d\Omega}{dt}\right)e^{i\Omega t} \qquad (9)$$

Equations (8) or (9) enable us to study the dynamics of shaft rotation with variable angular velocity Ω and to determine a method of easy crossing through a resonance region.

3. Dry Friction Damper

A nonlinear dry friction damper has been applied in the tail rotor drive shaft structure in order to ensure easy crossing through the resonance region. Its sketch is presented in Fig. 2.
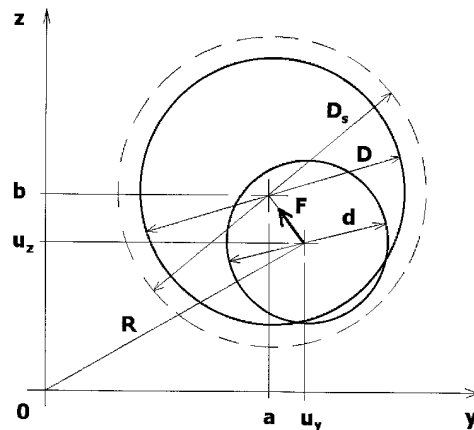

Fig.2. Sketch of the damper.

A disk with a central hole of D-diameter is the essential part of the damper. The disk is located in a housing, which causes a dry friction on both sides of the disk by means of the controlled

press. It results in a resisting force *f* of the damper.

The shaft passes through the central hole of the damper and there is a gap between the hole and the shaft

$$s = 0.5(D - d) \qquad (10)$$

where *d* is the shaft diameter.

The shaft can move the damper disk in the *yz*-plane after overcoming the resistance force *f*. Tangent friction between the rotating shaft and the damper disk is neglected in the damper model and it is assumed that the force *F* of interaction between the shaft and the damper is acting along the line conecting their centers (Fig. 2). The mass of the damper disk is also neglected.

It is assumed that the damper disk has an elastic zone of D_s diameter in which the force *F* is varying from zero to f (Fig.3).
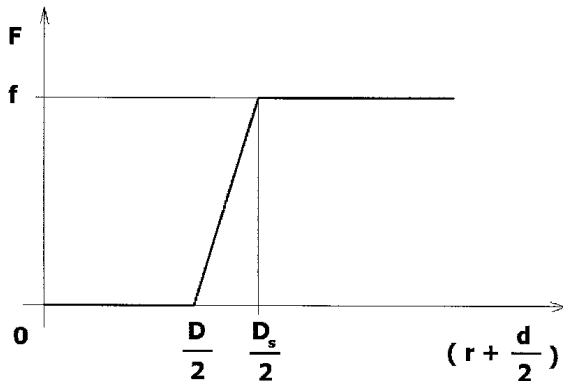
Fig.3. The force *F* of interaction.

The damper disk can move together with the shaft under its pressure when the force F has its maximal value.

The characteristic parameters of the damper are :

f	maximal force,
s = (D - d)/2	gap,
h = (D_s - D)/2	width of elastic zone,
a(0), b(0)	initial position.

The mathematical model of the damper is the following

$$r = \sqrt{(u_y - a)^2 + (u_z - b)^2} \qquad (11)$$

$$R = \sqrt{u_y^2 + u_z^2}$$

for $r + \dfrac{d}{2} > \dfrac{D_s}{2}$:

$$\begin{cases} F_y = f\dfrac{u_y - a}{r} \\[2mm] F_z = f\dfrac{u_z - b}{r} \\[2mm] a_t = a_{t-1} + \dfrac{1}{2}(2r + d - D_s)\dfrac{u_y - a_{t-1}}{r} \\[2mm] b_t = b_{t-1} + \dfrac{1}{2}(2r + d - D_s)\dfrac{u_z - b_{t-1}}{r} \end{cases} \qquad (12)$$

for $\dfrac{D}{2} \le r + \dfrac{d}{2} \le \dfrac{D_s}{2}$:

$$\begin{cases} F_y = f\dfrac{(u_y - a)(2r + d - D)}{r(D_s - D)} \\[2mm] F_z = f\dfrac{(u_z - b)(2r + d - D)}{r(D_s - D)} \end{cases} \qquad (13)$$

for $r + \dfrac{d}{2} < \dfrac{D}{2}$:

$$\begin{cases} F_y = 0 \\ F_z = 0 \end{cases} \qquad (14)$$

The force *F* is introduced into Eqs. (8), (9) as an additional edge force.

4. Simulation of the crossing through the resonance region

The crossing through the resonance region is investigated under assumption that the shaft is homogeneous and has the following parameters :

$L = 3.32$ m   length,
$\rho = 2700$ kg/m^3 density,
$A = 0.00022$ m^2 cross-sectional area,
$E = 0.7 \cdot 10^{11}$ Pa   Young modulus,
$I = 59.3 \cdot 10^{-9}$ m^4 moment of inertia,
$e = 0.001$ m   mass excentrity,
$c = 0.5$ Ns/m   external damping,
$k_p = 10^6$ N/m   rigidity of supports,
$c_p = 0$ Ns/m   damping in the supports.

The shaft is divided into four finite elements of the same length. Equations of motion (8) have been solved by means of the Runge-Kutta method.

In order to present the damper parameters and results of computation in a dimensionless form an approximated mass m_0 and rigidity k_0 of the shaft have been determined making use of Rayleigh method :

$$m_0 \approx 0.5\rho AL \; ; \; k_0 = \frac{48EJ}{L^3} \qquad (15)$$

It results that the first frequency of the shaft is:

$$\Omega_0 = \sqrt{\frac{k_0}{m_0}} \approx 74 \; rad/s \,. \qquad (16)$$

Dimensionless parameters of the damper are:

$$f* = \frac{f}{m_0\Omega_0^2 e} \; ; \; s* = \frac{s}{e} \; ; \; h* = \frac{h}{e} \,. \qquad (17)$$

Calculations have been performed for the following variants of the gap: $s* = 1, 2, 3, 4$.
It has been also assumed that:
$a(0) = b(0) = 0 \; ; \; h = f \cdot 10^{-5}$ [m]. $\qquad (18)$

Displacements of the shaft have been analyzed for the point located in the center o the shaft ($x/L = 0.5$). The damper was located in the same point (Fig.1). The velocity of rotation of the shaft was assumed as:

$$\Omega(t) = \Omega(0) + \varepsilon t = 10t \,. \qquad (19)$$

Results of calculations have been presented in the form of dimensionless displacement R/e depending on dimensionless velocity of rotation Ω/Ω_0 for variable parameters: $s*$, $f*$, $h*$. Results are presented in the next Figures.
In Fig.4 we can see the vibrations of the shaft without damper ($s* = f* = h* = 0$).
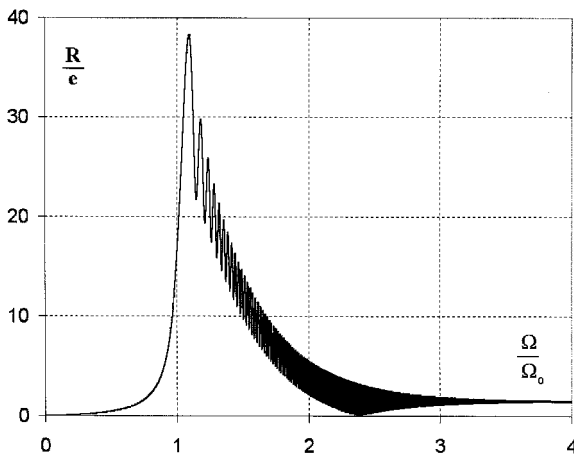
In the Figs. 5 to 10 we can see vibrations for the shaft with the damper without gap ($s* = 0$) and variable $f*$, $h*$.
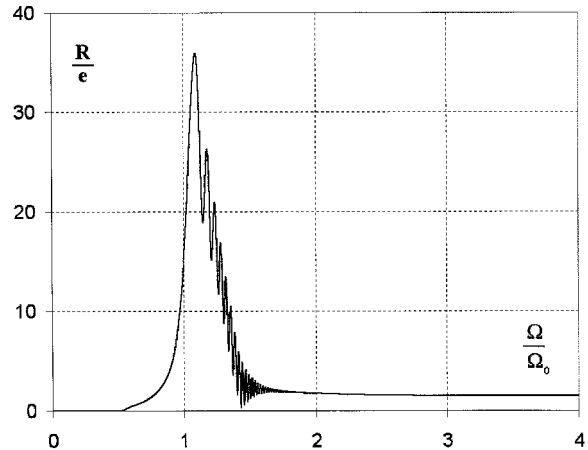
Fig.5 $s* = 0$; $f* = 0.183$; $h* = 0.01$.
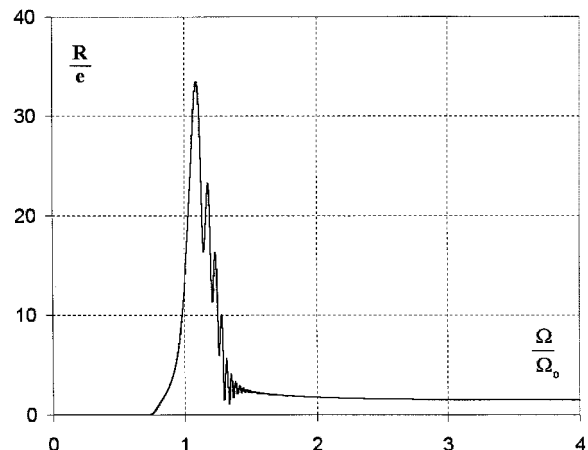
Fig.6 $s* = 0$; $f* = 0.367$; $h* = 0.02$.
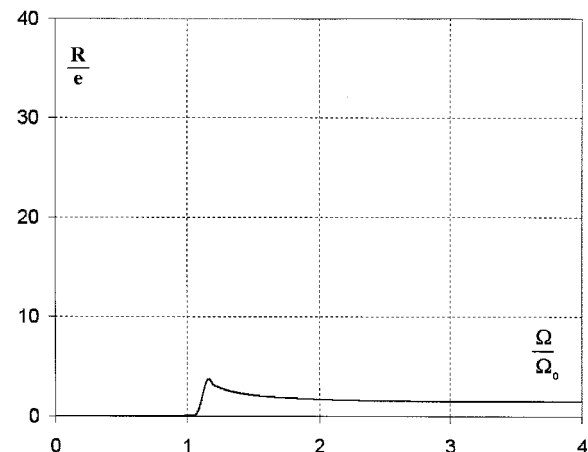
Fig.4 $s* = 0$; $f* = 0$; $h* = 0$.

Fig.7 $s* = 0$; $f* = 0.734$; $h* = 0.04$.

In the next Figs. 11 to 16 we can see the course of vibrations for the shaft with the damper with the gap $s* = 1$ and variable $f*$, $h*$.
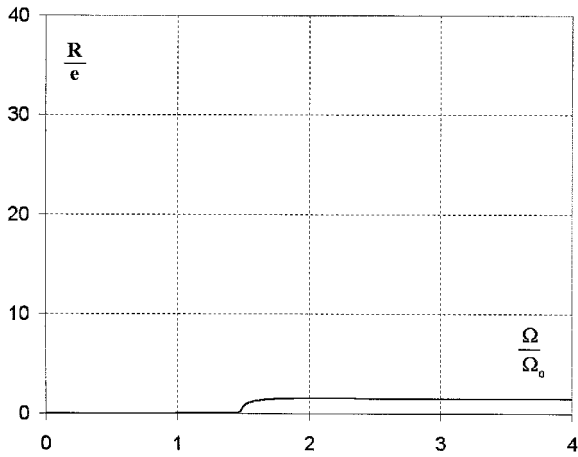
**Fig.8** $s* = 0$; $f* = 1.468$; $h* = 0.08$.
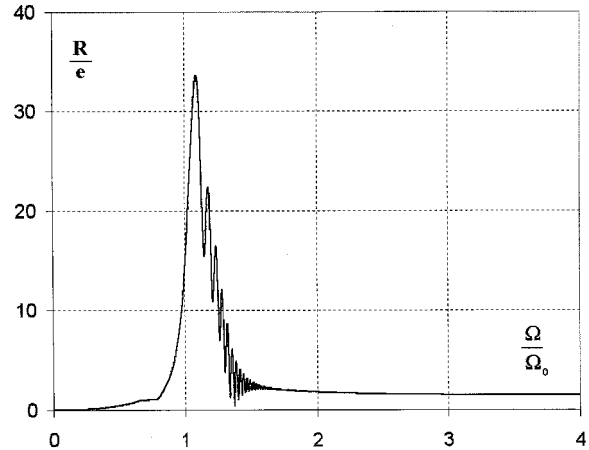

Fig.11 $s* = 1$; $f* = 0.183$; $h* = 0.01$.
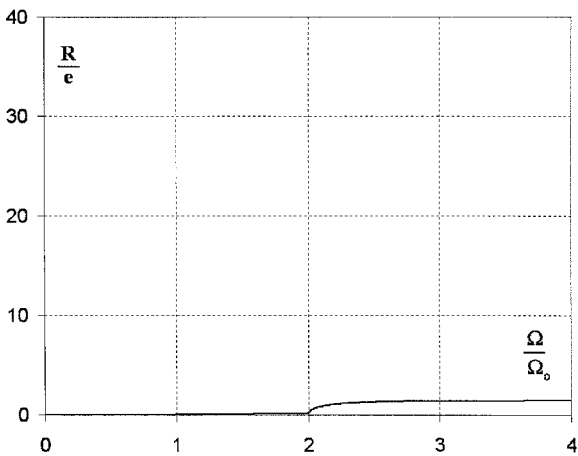
Fig.9 $s* = 0$; $f* = 2.935$; $h* = 0.16$.
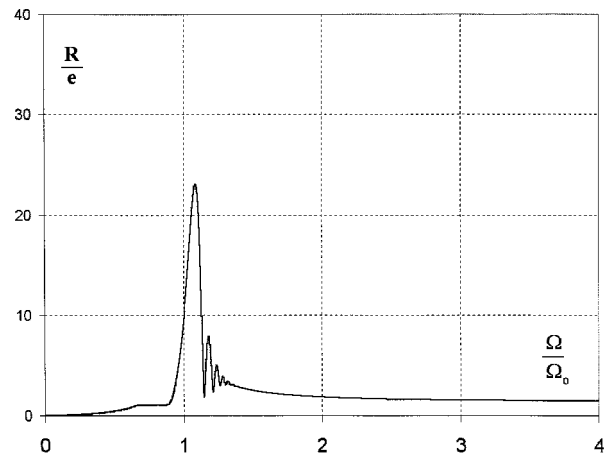
Fig.12 $s* = 1$; $f* = 0.367$; $h* = 0.02$.
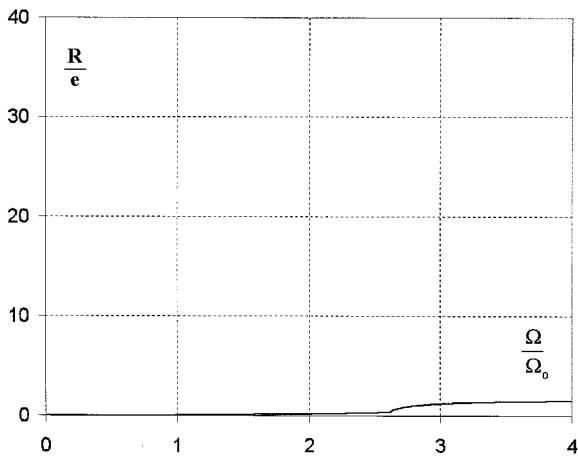
Fig.10 $s* = 0$; $f* = 5.871$; $h* = 0.32$.
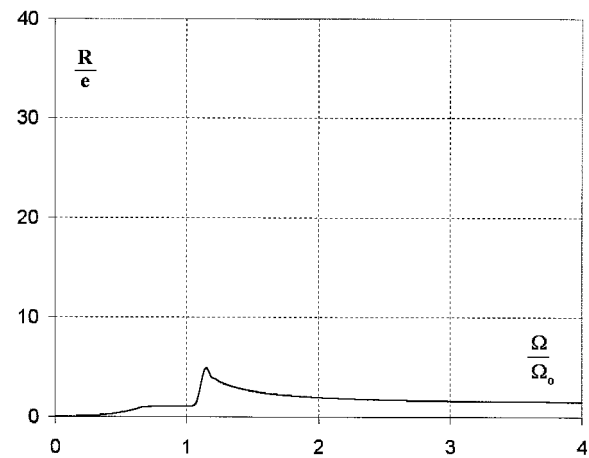
Fig.13 $s* = 1$; $f* = 0.734$; $h* = 0.04$.

In the Figs. 17 to 22 the shaft vibrations are presented for $s* = 2$ and variable $f*$, $h*$.
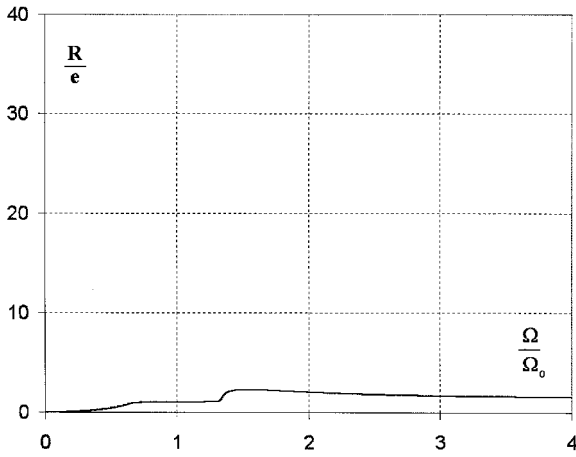
Fig.14 $s* = 1$; $f* = 1.468$; $h* = 0.08$.
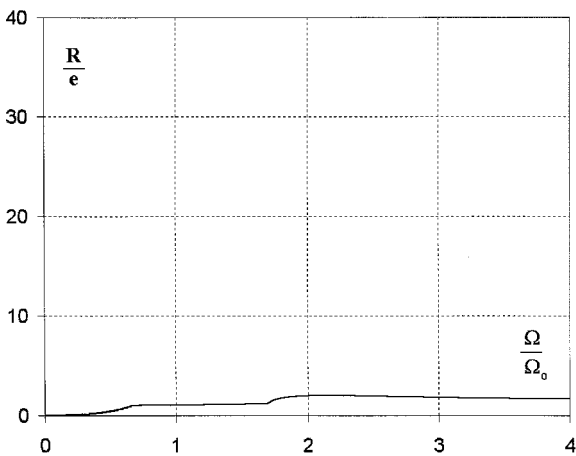
Fig.15 $s* = 1$; $f* = 2.935$; $h* = 0.16$.

Fig.16 $s* = 1$; $f* = 5.871$; $h* = 0.32$.

Fig.17 $s* = 2$; $f* = 0.183$; $h* = 0.01$.
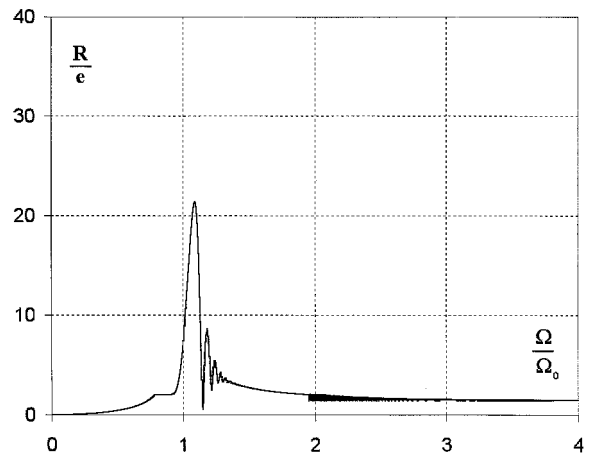
Fig.18 $s* = 2$; $f* = 0.367$; $h* = 0.02$.
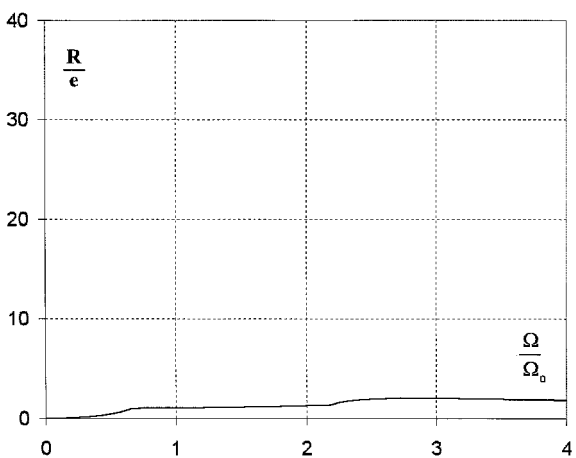
Fig.19 $s* = 2$; $f* = 0.734$; $h* = 0.04$.

In the next Figs. 23 to 28 the shaft vibrations are shown for $s^* = 4$ and variable f^*, h^*.
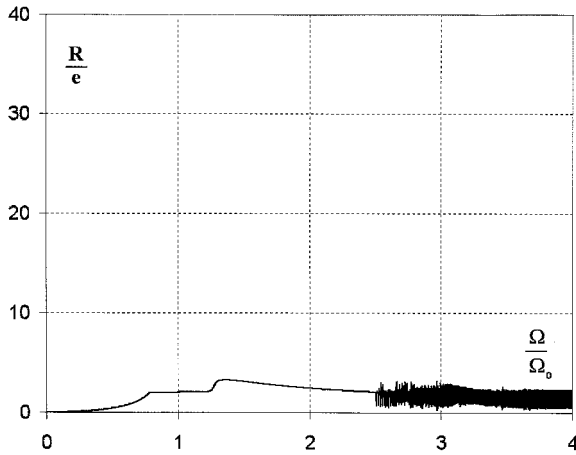

Fig.20 $s^* = 2$; $f^* = 1.468$; $h^* = 0.08.$
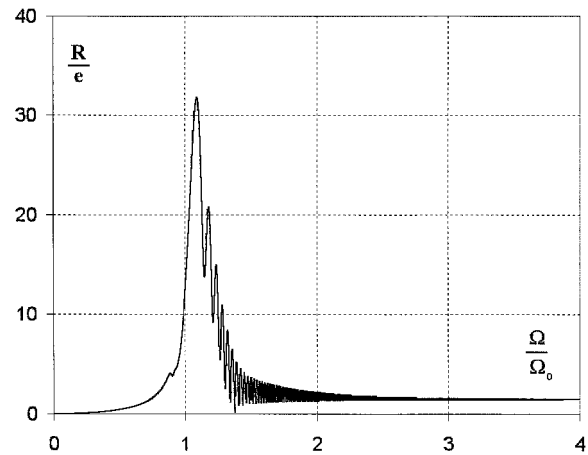
**Fig.23** $s^* = 4$; $f^* = 0.183$; $h^* = 0.01.$
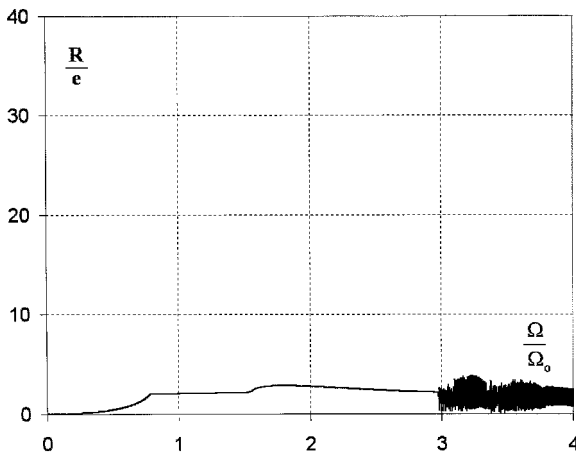
**Fig.21** $s^* = 2$; $f^* = 2.935$; $h^* = 0.16.$
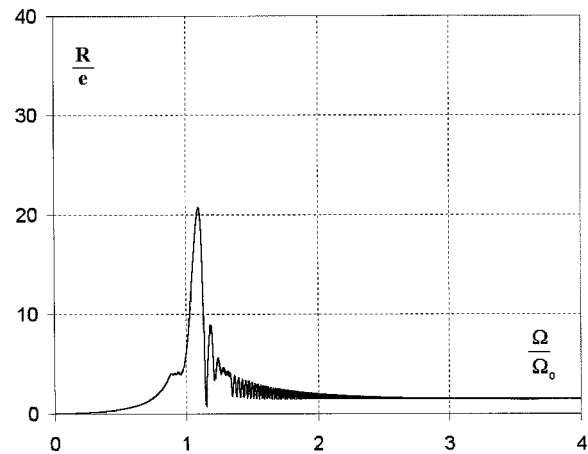
Fig.24 $s^* = 4$; $f^* = 0.367$; $h^* = 0.02.$
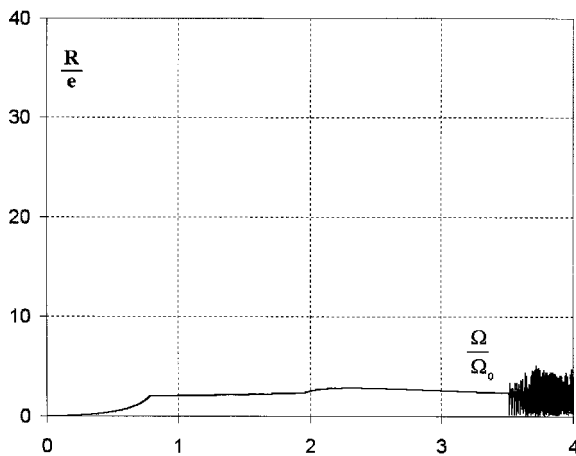

**Fig.22** $s^* = 2$; $f^* = 5.871$; $h^* = 0.32.$
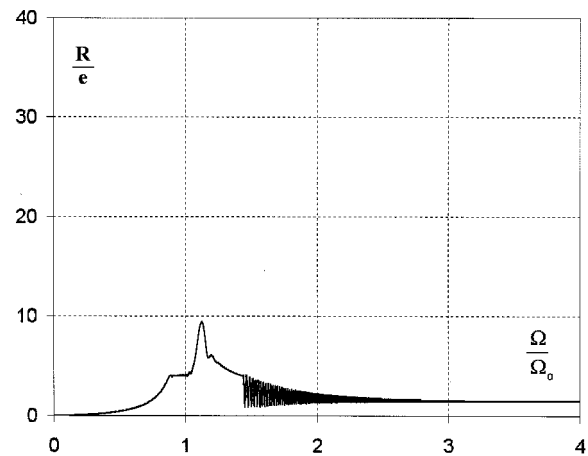
**Fig.25** $s^* = 4$; $f^* = 0.734$; $h^* = 0.04.$
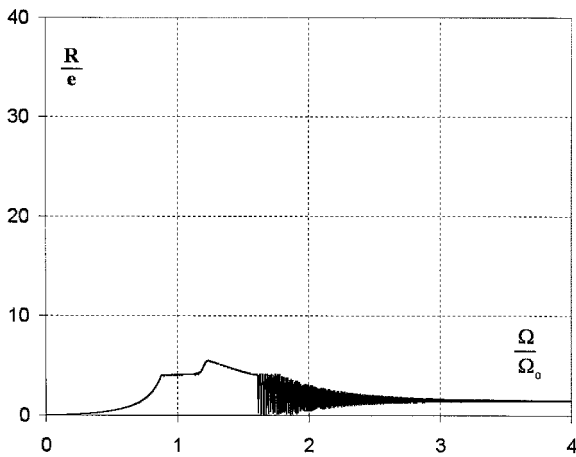
Fig.26 $s^* = 4$; $f^* = 1.468$; $h^* = 0.08$.
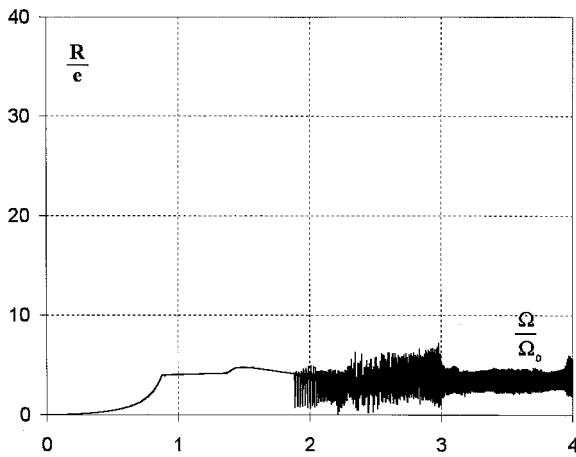

Fig.27 $s^* = 4$; $f^* = 2.935$; $h^* = 0.16$.
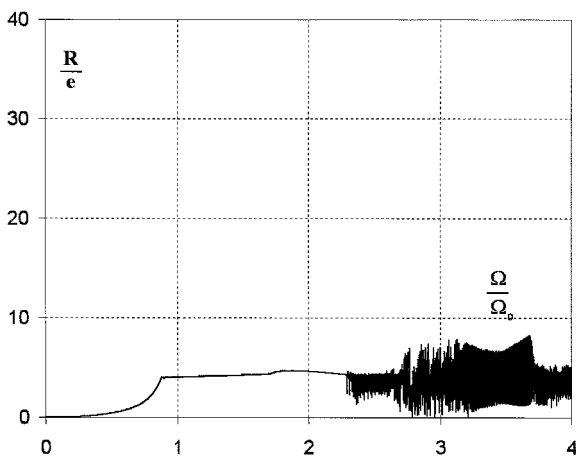
Fig.28 $s^* = 4$; $f^* = 5.871$; $h^* = 0.32$.

For sufficiently high values of the damper force f^* resonance peak can be completely destroyed. From these pictures we see that for sufficiently large gap and force and Ω/Ω_0 irregular vibrations can appear (Figs. 19,20,21,22,27,28). The course of these irregular vibrations is shown in Figs.29-31, for the data of Fig.27 and $\Omega/\Omega_0 = 2,5$.
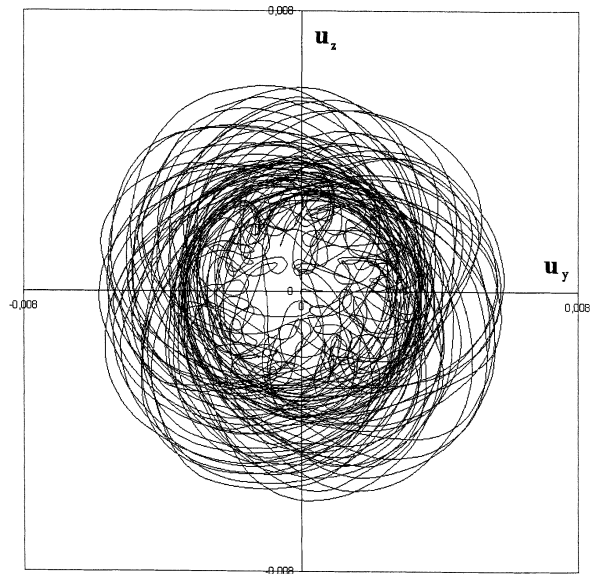

Fig.29 Trajectory of the shaft center for: $s^* = 4$; $f^* = 2.935$; $h^* = 0.16$; $\Omega/\Omega_0 = 2.5$; $\Delta t \approx 5$sec.
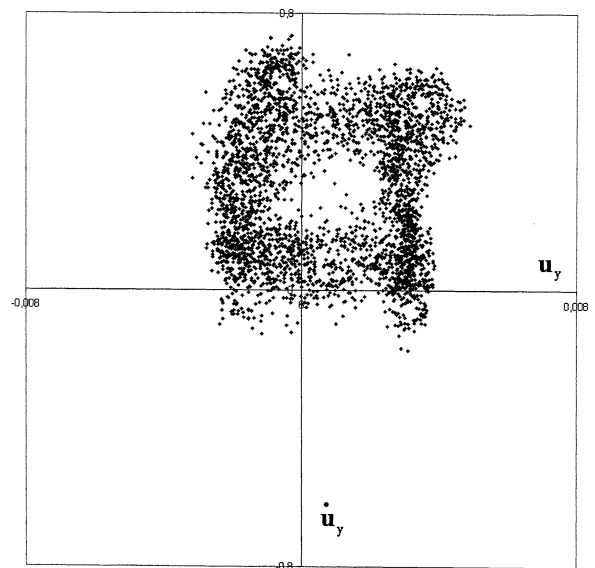

Fig.30 Poincare map for u_y ; $s^* = 4$; $f^* = 2.935$; $h^* = 0.16$; $\Omega/\Omega_0 = 2.5$.

From this pictures we can see that for small values of force f^* we have resonance peaks independent of gap s^* and width h^*.
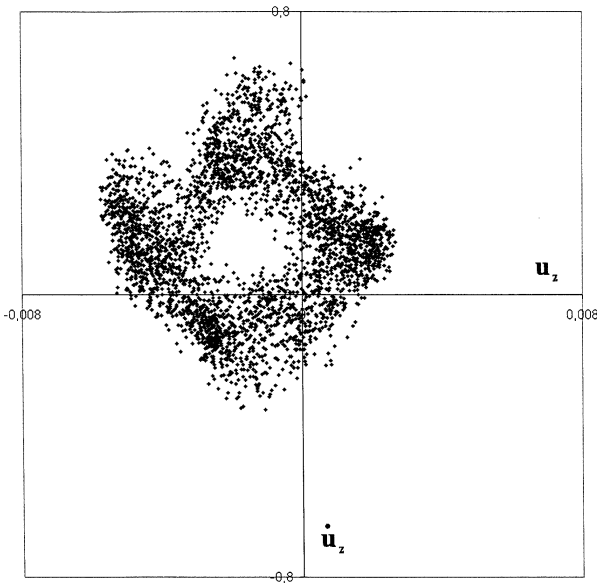
Fig.31 Poincare map for u_z ; $s^* = 4$; $f^* = 2.935$; $h^* = 0.16$; $\Omega/\Omega_0 = 2.5$.

From pictures in Figs. 29 to 31 we see that vibrations of the shaft center in this case are completely chaotic.

5. Conclusions

Results of analysis enable us to state that dry friction damper under investigation effectively limits the shaft vibrations during crossing through the resonance region and it increases critical velocity of shaft rotation. We can distinguish two characteristic cases:

1) for small gap $s^* < 1.5$,
2) for large gap $s^* > 1.5$.

Value of $s^* = 1.5$ is the border between two cases, because far away from the first resonance peak, the settled amplitude of mentioned shaft center equals $R/e \approx 1.5$ (Fig.4).

In the first case the shaft vibrations are regular but it has steady contact with the damper what is undesirable in practice.

In the second case for small values of force f^*, the shaft after resonance crossing, can rotate without contact with the damper. For greater values of f^* the contact with damper is steady and irregular vibrations can appear.

References

[1] Zienkiewicz O.C., Cheung Y. K. *The finite element method in structural and continum mechanics.* Mc Graw-Hill Publishing Company, London, New-York 1967.

[2] Dzygadlo Z., Finite element analysis of natural and forced flexural vibrations of rotor systems. *Jour. Tech. Phys.*, **21**, 1, 1980.

[3] Dzygadlo Z., Numerical analysis of flexural vibrations of rotors resting on elastic supports. *Jour. Tech. Phys.*, **22**, 4, 1981.

[4] Guckenheimer J., Holmes P. *Nonlinear oscillations, dynamical systems, and bifurcations of vector fields.* Springer-Verlag, New York, Berlin 1983.

[5] Ott E. *Chaos in dynamical systems,* Cambridge University Press, 1993.

[6] Bogusz W., Dzygadlo Z., Rogula D., Sobczyk K., Solarz L. *Vibrations.* PWN, Elsevier, Warsaw, Amsterdam 1992.